

OPTICAL PROPERTIES OF DIAMOND

Diamond offers unique properties for optical elements and coatings. This article reviews the properties of diamond and presents the results of recent measurements and efforts in the modeling of its optical properties at the Applied Physics Laboratory.

INTRODUCTION

In the past, the commercial use of diamonds was restricted to poor optical quality "industrial diamonds" for cutting and grinding. These diamonds were either natural diamonds unsuitable for gems or were manufactured by subjecting graphite, the stable form of carbon at ambient conditions, to intense pressure and temperature. The use of diamond as an optical material was restricted to a few specialized applications such as planetary radiometry from satellites (e.g., Nimbus and the Pioneer series) and high-pressure cells ("diamond anvils"). Recent progress in the manufacture of high-quality diamonds through the chemical vapor deposition (CVD) process opens the possibility of their use in new commercial applications, including semiconducting diamond electronic devices, diamond substrates as heat sinks, and durable optical elements with wide transmission ranges.

Diamond is thermodynamically unstable at pressures below 1.2 gigapascals (GPa), but conversion to graphite is extremely slow at temperatures below 1500 K. Diamond synthesis was first performed by the General Electric Company in 1955 using pressures of 4.5 to 6 GPa and temperatures of 1600 to 1900 K, which are thermodynamically stable conditions for diamond. Molten metal catalysts cause diamond to form at practical rates at these relatively low (for carbon) temperatures. Non-catalytic diamond synthesis requires higher temperatures (≥ 2500 K) and pressures (~ 10 GPa). These conditions typically yield micrometer-sized diamond powder, but gem-quality single crystals can be grown.¹

Development of new CVD diamond growth techniques began in the early 1980s by the Japanese and, by the end of the decade, it became possible to make large structures of high-quality polycrystalline diamond²⁻³ whose mechanical,⁴ thermal,⁵⁻⁷ and optical properties approach those of Type IIa natural diamonds (see the boxed insert). A major advantage of the CVD technique is that growth can occur at lower temperature (~ 1200 K) and very low pressure (2500 Pa). Films are grown on a temperature-controlled, heated substrate, such as silicon, metal oxides, or refractory metals, using methane or acetylene (mixed with hydrogen and other gases) as a source of carbon (CH_3 is the active radical). Microwaves, hot sparks, hot filaments, or other techniques are used to dissociate the gases partially. The various CVD techniques produce high-quality polycrystalline diamond films

TYPES OF DIAMONDS

Four classifications of natural diamond have been made on the basis of optical properties. Only Type IIa is suitable for infrared optics.

Type Ia accounts for 95 to 98% of natural diamond and contains substantial nitrogen impurity (up to 0.2%), which forms in aggregates or platelets. This type of diamond has strong absorption below 320 nm, low thermal conductivity (< 9 W/[m·K]), and high electrical resistivity ($> 10^{14}$ Ω -m).

Type Ib also has substantial nitrogen but in a dispersed substitutional form. The nitrogen imparts color, ranging from pale yellow to green, depending on nitrogen concentration. Synthetic industrial diamonds are typically Type Ib.

Type IIa is gem-quality diamond essentially free of nitrogen. This type has the highest thermal conductivity (> 2000 W/[m·K]), high electrical resistivity ($> 10^{14}$ Ω -m), and good optical transmission.

Type IIb is also nitrogen-free but contains boron impurity (up to 0.25 ppm in natural diamond and up to 270 ppm in doped synthetic diamond) that results in *p*-type conductivity (electrical resistivity 0.1 to 100 Ω -m) and imparts a blue color to the diamond.

(Fig. 1). These films have great promise for optical (infrared) elements and hard optical coatings.

Our interest in CVD diamond is principally as a long-wavelength optical window for infrared sensors. Diamond offers extreme hardness and strength, excellent transparency, resistance to chemical attack, performance at higher temperatures, and better thermal shock capability compared with other long-wavelength window materials such as zinc sulfide, zinc selenide, and gallium arsenide.

PROPERTIES OF DIAMOND

The unique properties of pure (Type IIa) diamond⁸ arise primarily from its structure. Diamond has a face-centered, cubic, close-packed structure with the greatest atomic number density of any material (1.76×10^{23} atoms/cm³). The individual carbon-carbon bonds are not especially strong, but the tetragonal symmetry and high coordination number of cubic Group IV elements (carbon, silicon, and germanium) impart unusual stiffness, strength, and hardness through the number and symmetry of the bonds and close packing of light atoms. Table 1



Figure 1. Polycrystalline diamond windows made by Norton (DiamaTorr process). The square windows are 1 in. on a side and are polished; the 4-in. circular wafer is unpolished. All samples are about 0.5-mm thick. The slight brown coloring is due to scatter. (Photograph courtesy of the Norton Diamond Film Company.)

compares the hardness of diamond with other very hard materials. Diamond is the stiffest, strongest, and hardest known material by at least a factor of 2.⁸

In addition to diamond's unique mechanical properties, its thermal properties are also unusual. The strong net bonding results in very low thermal expansion, high acoustic frequencies (and hence a very high Debye temperature of 2220 K), and low room-temperature heat capacity. Even more remarkable is the exceptionally high room-temperature thermal conductivity of diamond, which is more than five times that of metals such as silver or copper. This large thermal conductivity results in high resistance to thermal shock and thermal lensing.

Table 2 compares the thermal conductivity of natural diamonds and CVD diamonds. Thermal conductivity is a strong function of impurities (especially nitrogen), defect concentration, and isotopic content. Recent research on the thermal conductivity of diamond shows a 50% increase when ¹³C content is reduced to 0.1% (from its natural 1.1% abundance).^{1,9} The thermal conductivity of recently developed thick polycrystalline diamond films approaches that of a single crystal.

Type IIa diamond is an excellent insulator and is resistant to chemical attack at ordinary temperatures. Diamonds heated above 875 K in the presence of oxygen or other catalytic agents form a graphite surface coating. Oxidation rates are 0.1 μm/h at 600°C and 4 μm/h at 700°C.¹² In vacuum, significant conversion to graphite ("graphitization") requires temperatures above 1800 K.

Table 3 summarizes the properties of Type IIa diamond. Additional electronic, lattice, and transport properties are presented in standard handbooks.²¹

OPTICAL PROPERTIES OF DIAMOND

Diamond's structure contributes to its unique optical properties, and its symmetry results in a pure covalent bonding, which accounts for the absence of infrared

Table 1. Comparison of the Knoop hardness of diamond with that of other hard materials.⁸

Material	Hardness (kg/mm ²)
Diamond	9000
Boron nitride	4500
Boron carbide	2250
Tungsten carbide	2190
Sapphire	2000

Table 2. Thermal conductivity of diamond.

Type	Thermal conductivity (W/[m·K])
Natural, IIa ^{10,11} (or artificial)	2000 to 2300
Natural, Ia ^{1,8,10,11} ($1.7 \times 10^{20}/\text{cm}^3$ N)	800
Artificial, ^{1,9} (99.9% ¹² C)	3320
CVD ⁵⁻⁷	1280 to 1700

optical activity (no interaction of light with lattice vibrations). To first order, diamond is transparent from its (indirect) electronic band gap (at 225 μm) to the microwave region. Higher-order (multiphonon) lattice absorption processes cause significant absorption in the 2.5- to 6-μm region. Diamond has a Raman-active optical mode²² (F_{2g} or Γ⁽²⁵⁺⁾ symmetry) at 1332.4 cm⁻¹ (7.505 μm). A sharp Raman line indicates high-quality diamond and is used as a qualitative measure of CVD films, al-

Table 3. Room temperature properties of Type IIa diamond.

Property	Value
Space group	Fd3m (O_h^7)
Lattice constant ¹³	0.356683 nm ($Z = 8$)
Density ¹⁴	3.51525 g/cm ³
Elastic moduli ^{15,a}	$c_{11} = 1076.4$ GPa $c_{12} = 125.2$ GPa $c_{44} = 577.4$ GPa
Engineering moduli (random average)	elastic: 1143 GPa shear: 535 GPa bulk: 442 GPa
Poisson's ratio	0.0691
Knoop hardness ⁸	9000 kg/mm ² (500 g)
Strength ⁸	2500 to 3000 MPa
Melting point ¹⁶	4100 K ($P = 12.5$ GPa)
Debye temperature ⁸	2200 K
Heat capacity ¹⁷	6.195 J/(mol·K)
Thermal expansion ¹⁸	$0.8 \times 10^{-6}/K$
Thermal conductivity ^{10,11}	2300 W/(m·K)
Band gap, ¹⁹	5.50 eV
Refractive index, ²⁰ n_D	2.41726
Abbe number, ^b ν_D	55.3
Dielectric constant, ²⁰ ϵ	5.70
	$(d\epsilon/dT)_P = 4.61 \times 10^{-5}/K$ $(d\epsilon/dP)_T = -4.1 \times 10^{-12}/Pa$

Note: Z = number of atoms in a unit cell.

^aPressure and temperature dependence of the elastic constants can be found in H. J. McSkimin and P. Andreatch, "Elastic Moduli of Diamond as a Function of Pressure and Temperature," *J. Appl. Phys.* **43**, 2944-2948 (1972).

^bReference 8, p. 650, gives refractive indices $n_C = 2.40990$, $n_D = 2.41726$, $n_F = 2.43554$, and $\nu_D = 55.3$; source is unknown.

though small grain size ($<\lambda_{\text{Raman}}/2$) reduces Raman intensity.²³ Nondiamond character is usually revealed by Raman response² near 1550 cm⁻¹.

Visible Properties

The refractive index n of diamond²⁴⁻²⁶ is given by the Sellmeier equation,²⁴

$$n^2 - 1 = \frac{4.3356\lambda^2}{\lambda^2 - (0.1060)^2} + \frac{0.3306\lambda^2}{\lambda^2 - (0.1750)^2}, \quad (1)$$

where the wavelength λ is in micrometers. This equation can be used to determine reflectivity from 0.225 μm (in the ultraviolet) through the infrared. Note that diamond has a high index of refraction with high dispersion in the visible (which is enhanced by the cut of diamond gems) and essentially no dispersion in the infrared.²⁵

The temperature derivative of the refractive index (thermo-optic coefficient) is available for visible wavelengths²⁷ and at low frequency²⁰ and is given in Table 4.

Color in diamond comes from impurities. Nitrogen and boron are the principal impurities and impart yellow and blue coloring, respectively, when they are in sufficient concentration. The nitrogen impurity can take several forms: single-substitution as well as distinct types of precipitates ("platelets"). Nitrogen causes an increased lattice constant, increased ultraviolet (e.g., at 0.3065 μm)

and infrared (e.g., at 7.8 μm) absorption, slight birefringence, and decreased thermal conductivity.¹³ Metals such as iron, aluminum, magnesium, and others are believed to cause green and brown coloration. Type IIa diamonds are clear with very low concentrations of nitrogen (≤ 20 ppm), boron, and other impurities.

Optical scatter in single-crystal Type IIa diamonds is very low. Polycrystalline CVD diamond has higher scatter caused by grain boundaries. Grain size and surface polish determine the scatter level in CVD diamond, and scatter can significantly limit transmission in the visible, ultraviolet, and near-infrared regions.²⁸ Scatter in CVD diamond is recognized by a gray or brown cast to the sample and by uniformly decreasing transmission at high frequency.

Ultraviolet Properties

Figure 2 shows an APL measurement of the ultraviolet transmission of a Type IIa diamond window (0.5-mm thickness) in the region near its band gap. The extinction coefficient also shown in Figure 2 is derived using the index of refraction from Equation 1 and solving the resulting quadratic equation that relates the absorption coefficient to transmittance. The exponential increase in absorption with frequency (or energy) near the band gap (5.5 eV) is known as the Urbach edge. The ultraviolet absorption coefficient β can be modeled as a function of energy E (in eV) and temperature T by the equation

$$\beta(E, T) = \beta_0 \exp\left[\frac{\sigma(T)(E - E_0)}{k_B T}\right], \quad (2)$$

where k_B is Boltzmann's constant.

Using the room-temperature absorption data of Figure 2 and assuming a value of 6.5 eV (the direct band gap) for the constant E_0 of Equation 2, gives the following parameters for the Urbach edge model: $\beta_0 = 4.23 \times 10^{11}$ cm⁻¹, $\sigma(300\text{ K}) = 0.585$. Temperature-dependent absorption measurements are needed to derive the temperature dependence of $\sigma(T)$ and give the precise location of E_0 .

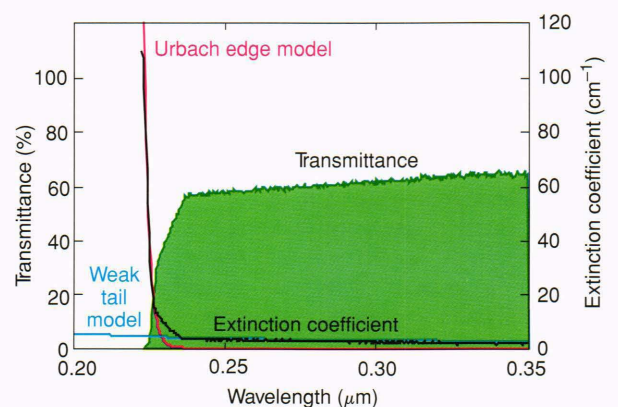


Figure 2. Our measurement of the ultraviolet transmission and absorption coefficient of Type IIa diamond (0.5-mm thick) at room temperature. The gradually rising absorption (weak absorption tail) becomes rapid (Urbach absorption edge) at the band gap (225 nm). Both types of absorption can be described by exponential functions.

Table 4. Temperature derivative of the refractive index n of diamond.

Wavelength (μm)	Refractive index	$(dn/dT) \times 10^{-6}/\text{K}$	$(1/n)dn/dT \times 10^{-6}/\text{K}$	Ref.
0.4358	2.4499	11.4	4.65	27
0.5461	2.4237	10.1	4.17	27
0.5893	2.4173	9.8	4.05	27
Long	(2.39)	9.6	4.04	20

The featureless extinction between 0.225 and 0.35 μm is believed to be caused by absorption rather than scatter.⁸ This absorption is also approximately exponential with energy and can be modeled as

$$\beta(E) = 0.28 \exp(0.45E), \quad (3)$$

where E is again in eV and the absorption coefficient is in cm^{-1} . This equation is in the usual form of the temperature-independent “weak-tail” absorption observed in crystalline and semiconductor materials.

Infrared Properties: Measurements

Our major interest in the optical properties of diamond is the significant multiphonon absorption region (see the boxed insert) that lies between 2.5 and 6 μm . This absorption limits the usefulness of diamond windows in the middle infrared region frequently used by infrared sensors. Measurements were made of natural, single-crystal Type IIa diamonds provided to us by the U.S. Army Strategic Defense Command (Figure 3). Figure 4 shows the room temperature absorption coefficient of diamond derived from transmission measurements. This figure clearly shows two-, three- and four-phonon absorption. We believe Figure 4 documents the first observation of four-phonon absorption in diamond. The triangle marks absorption measured by laser calorimetry,²⁹ which is used to calibrate the spectral transmittance. Also shown are our models of the absorption coefficient, which are discussed in this section.

Absorption at the infrared edge of insulators is caused principally by anharmonic terms in the lattice potential. These higher harmonics of the lattice resonances are infrared active even if the fundamental vibrations are not. This phenomenon is called multiphonon absorption because the light is absorbed by exciting multiple (two or more) lattice phonons (vibrations). For infrared absorption, each successively higher multiple of the fundamental frequency is weaker (and broader), leading to decreasing absorption beyond the highest fundamental absorption frequency (the maximum transverse optical phonon frequency). The resulting infrared absorption edge of most materials (especially highly ionic insulators) is characterized by an absorption coefficient that decreases exponentially with frequency. At about three times the highest transverse optical frequency, the absorption coefficient becomes reasonably small, and a material with a thickness from 1 to 10 mm is basically transparent.

Group IV materials with the diamond structure are unique in that no infrared-active fundamental lattice vibrations are present: to first order, the material is transparent throughout the infrared. Higher-order (mul-

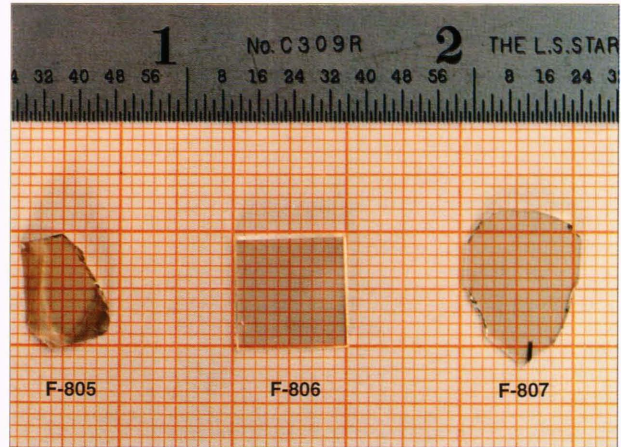


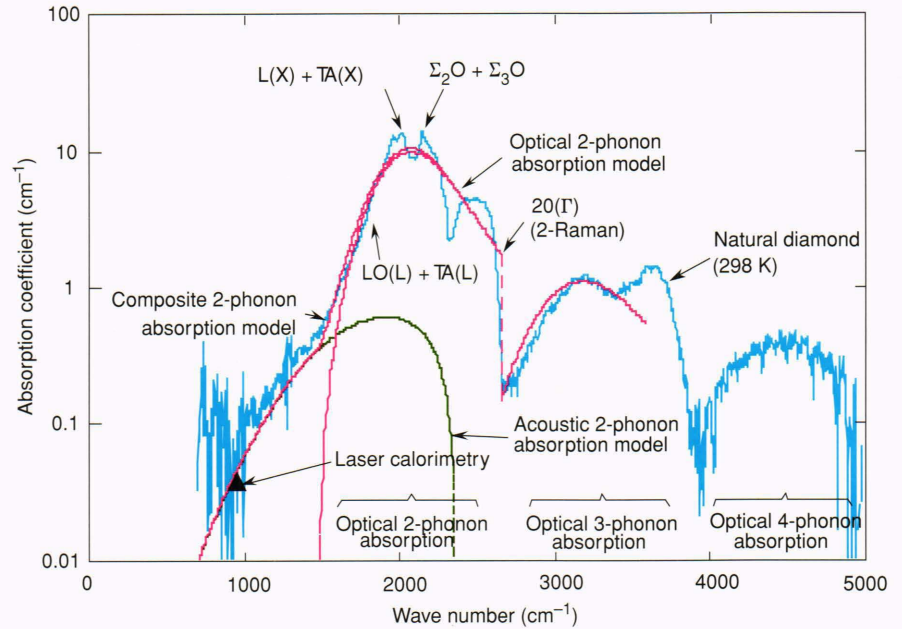
Figure 3. Natural Type IIa diamonds supplied by the U.S. Army Strategic Defense Command for characterization. Sample F-805 (left) is 9.5-mm long, has a clear aperture of 4 mm, and weighs 0.150 g. Sample F-806, used for the measurements reported here, is 10-mm square, 0.5-mm thick, and weighs 0.166 g. Sample F-807 is 13.8-mm long, 0.32-mm thick, weighs 0.104 g, and has a small crack (dark area) at the bottom. (One carat equals 0.2 g.)

tiphonon) absorptions are, however, optically active and, in diamond, cause considerable absorption in the 2.5- to 6- μm (1700- to 4000- cm^{-1}) spectral region.

Figure 5 shows absorption in the 10- μm region. This measurement was made using a longer integration time than was used for Figure 4. The longer integration time improves the signal-to-noise ratio at the expense of absolute accuracy. These data have been corrected using well-established features from short integration time measurements. The absorption features seen are real; they arise from the intrinsic vibrational modes of diamond activated by defects and impurities and possibly by infrared bands associated with defect centers and substitutional impurities. Many of these features can be correlated with zone-edge critical-point phonon vibrations³⁰ visible in Figure 5. The triangle marks absorption measured by laser calorimetry (also shown in Fig. 4).

We have also measured the temperature dependence of the infrared absorption coefficient. As temperature increases, the multiphonon absorption becomes stronger and reaches the classical limit of T^{n-1} at high temperature, where n ($\approx \nu/\nu_{\text{Raman}}$) is the number of phonons contributing to absorption. At low temperature, absorption has no temperature dependence, since only transitions from the ground state occur. Once the temperature is sufficiently high (i.e., approaching the Debye temperature), transitions that originate from excited states become important, and the classical temperature depen-

Figure 4. Our measurement of the infrared absorption coefficient of Type IIa diamond at room temperature. The two-, three-, and four-phonon absorptions in the 1000- to 5000-cm⁻¹ (2- to 10-μm) spectral region are clearly seen. Some two-phonon spectral features are labeled with their spectroscopic identification (e.g., L[x] is the longitudinal frequency at the X critical point).³⁰ These features, predicted by theory, are observed at the expected locations. Also shown are the optical and acoustic components of our multiphonon absorption model and a laser calorimetry measurement (triangle).²⁹



ABSORPTION IN SOLIDS

The absorption of light in insulating solids arises from two principal sources: electronic transitions and lattice vibrations. Electronic absorption typically occurs in the ultraviolet, whereas absorption by lattice vibrational modes occurs in the infrared.

A *phonon* is a quantum of lattice vibration (elastic energy) (as the *photon* is the quantum of electromagnetic energy). Phonons are classified as either acoustic (compression waves) or optic. Optic phonons that are *infrared active* absorb light through an interaction between the electric field of the light and the dipole moment of the material. Diamond is a symmetric, covalent material with no dipole moment and therefore has no infrared active phonons.

Weak phonon absorption can be induced in solids by very intense light (*Raman-active phonons*) or by combinations of phonons (*multiphonons*) that create weak dipole moments. Diamond has one Raman mode (observed at 1332.4 cm⁻¹) and one acoustic mode.

In crystals, frequencies of these modes change with propagation direction, creating many two-phonon absorption features. These multiphonon absorption bands are weak compared with fundamental (one-phonon) absorption and occur at frequencies that are harmonics of the fundamental frequency.

In diamond, which has no infrared-active one-phonon absorption, multiphonon effects dominate infrared absorption.

dence is observed. Figure 6 shows measured absorption coefficients at room temperature and at 771 K. Table 5 summarizes the band-integrated results for several temperatures. These absorption data are shown in Figure 7 compared with the classical temperature dependence. Note that the higher multiphonon contributions grow more rapidly with temperature as expected but have not reached a temperature where the classical limit applies.

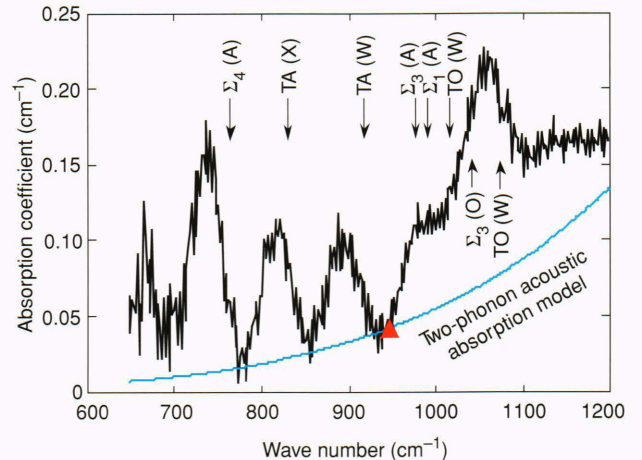


Figure 5. Room-temperature absorption in the 10-μm (1000 cm⁻¹) region. A longer integration time was used to reduce the noise seen in Figure 4. The various absorption features are caused by fundamental vibrational modes of diamond that would normally not be observed unless activated by defects and impurities. Some of these zone-edge critical-point vibrations are identified by their spectroscopic notation, as in Fig. 4.³⁰ Also shown is the laser calorimetry measurement (triangle) from Figure 4.²⁹

Another noticeable feature of the higher temperature data is the shift of the absorption bands to lower frequency. This red shift is caused by the increased population of higher energy levels coupled with the lower energy separation of these higher levels.

Chemical vapor deposition diamond has additional absorption features in the one-phonon region (500 to 1332 cm⁻¹) caused by greater concentration defects and impurities.³⁰ The optical (infrared) quality of diamond can be assessed by directly measuring absorption. As CVD techniques have improved, infrared absorption in CVD diamonds has approached that of natural diamonds.

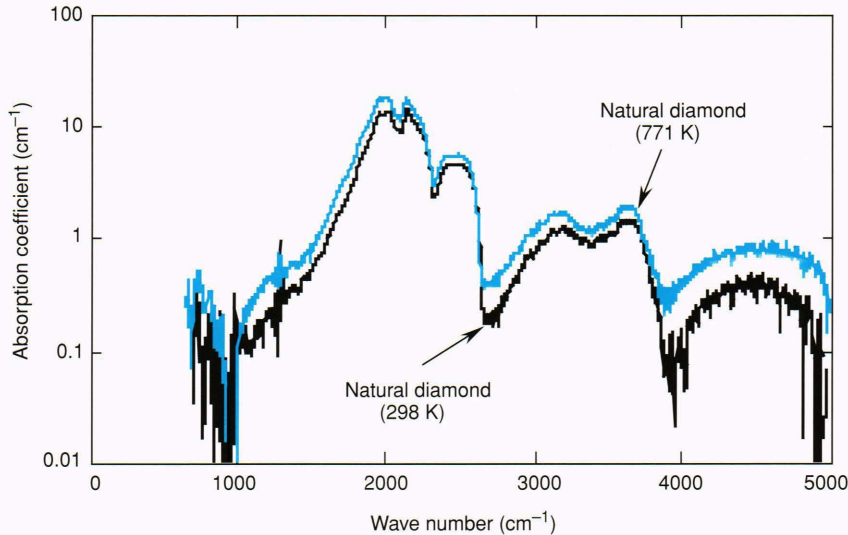


Figure 6. Temperature dependence of the infrared absorption coefficient. The blue curve shows room temperature absorption, and the green curve shows the absorption coefficient at 771 K. Note the red shift of the absorption spectra at high temperature and the more rapid growth of the strength of the higher-order multiphonon bands.

Infrared Properties: Models

We have successfully developed a semiempirical, quantum mechanical model of (sum-band) multiphonon absorption based on the Morse interatomic potential and a modified Gaussian function for the phonon density of states.³¹ Use of the Morse potential leads to an exact solution to the Schrödinger equation that includes anharmonic effects to all orders. The central limit theorem ensures that the phonon density of states becomes Gaussian for high-order multiphonon absorption. Our model contains parameters derived from room temperature measurements of absorption, it is computationally efficient, and it has been successfully applied to many ionic substances.³² Surprisingly, this model can also be applied to diamond.³³ Figure 4 shows the result.

Our multiphonon model is based on only six parameters: a dissociation energy (the depth of the Morse potential well), the maximum longitudinal optical phonon frequency, an absorption scaling constant, and three parameters that describe the phonon density of states. No optically-active modes are present in diamond; therefore, no maximum longitudinal frequency exists for the model. Instead, we use the Raman frequency and note the sharp decrease in absorption at two, three, and four times the Raman frequency (Fig. 4). Our multiphonon optical model cannot accurately reproduce the spectral content of the two-phonon region, which consists of many different two-phonon interactions,³⁰ because diamond does not conform to the near-Gaussian density of states assumption that becomes accurate only when several phonons interact (typically, three or more phonons). Some of the two-phonon spectral features are labeled in Figure 4.

Diamond absorbance near $10\ \mu\text{m}$ ($1000\ \text{cm}^{-1}$) is of particular interest because many infrared sensors operate at this wavelength. Evidence indicates that the absorption edge bounding this region is caused by two-phonon acoustic-acoustic interactions. Normally, pure acoustic multiphonon absorption is not measurable because it is obscured by strong one-phonon absorption. Diamond has

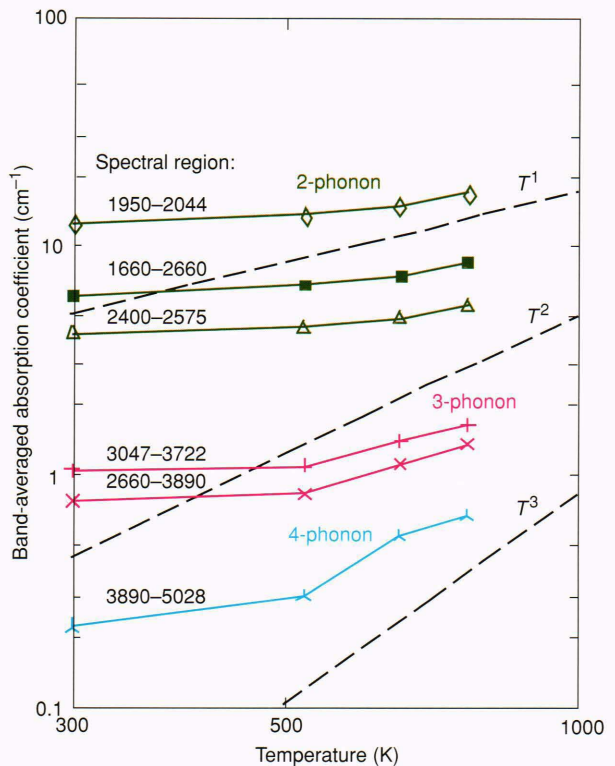


Figure 7. Temperature dependence of band-averaged infrared absorption coefficient for two-, three-, and four-phonon regions. Dashed curves show the T^{n-1} absorption dependence predicted by classical theory for high temperatures (n is the order of the phonon contribution). Lower signal-to-noise ratio accounts for the irregularity of the four-phonon result.

very high acoustic frequencies because of its strong bonds, and the lack of fundamental absorption unmasks the pure acoustic contribution. We model this contribution by assuming a Debye acoustic single-phonon distribution $\rho_1(\omega)$ of the form

Table 5. Band-averaged, temperature-dependent absorption coefficient (in cm^{-1}) of natural diamond from transmission measurements.

Absorption type	Spectral band		Temperature (K)			
	cm^{-1}	μm	298	522	656	771
Two-phonon	1660-2660	3.76-6.02	6.02	6.72	7.40	8.48
	1950-2044	4.89-5.13	12.23	13.73	15.01	16.97
	2400-2575	3.88-4.17	4.17	4.50	4.91	5.55
Three-phonon	2660-3890	2.57-3.76	0.77	0.84	1.12	1.38
	3047-3722	2.69-3.28	1.05	1.11	1.41	1.66
Four-phonon	3890-5028	1.99-2.57	0.22	0.30	0.55	0.67

$$\rho_1(\omega) = \begin{cases} \frac{3\omega^2}{\omega_{\max}^3} & (0 \leq \omega \leq \omega_{\max}) \\ 0 & (\omega > \omega_{\max}), \end{cases} \quad (4a)$$

where ρ is the density of states distribution function for acoustic modes, ω is the angular frequency, and ω_{\max} is found by fitting to data. Higher-order (n th) acoustic phonon distributions are computed by convolving this distribution with the $n - 1$ phonon distribution:

$$\rho_n(\omega) = \int_0^{\omega} \rho_{n-1}(\omega') \rho(\omega - \omega') d\omega'. \quad (4b)$$

For the two-phonon distribution, the result is

$$\rho_2(\omega) = \begin{cases} \frac{9}{\omega_{\max}^6} \left\{ \frac{\omega^2}{3} [\omega_{\max}^3 - (\omega - \omega_{\max})^3] - \frac{\omega}{2} [\omega_{\max}^4 - (\omega - \omega_{\max})^4] + \frac{1}{5} [\omega_{\max}^5 - (\omega - \omega_{\max})^5] \right\} & (\omega_{\max} \leq \omega \leq 2\omega_{\max}) \\ \frac{0.3\omega^5}{\omega_{\max}^6} & (0 \leq \omega \leq \omega_{\max}). \end{cases} \quad (4c)$$

Using the parameter $\omega_{\max} = 1183 \text{ cm}^{-1}$ and an absorption scaling constant of 487.5 cm^{-2} gives the result shown in Figure 4. This second (acoustic) contribution, although weak, is important because it lies in the 8- to 10- μm atmospheric window frequently used by infrared sensors. Note that our selected value of 1183 cm^{-1} is consistent with both the computed Debye frequency as well as the highest reported acoustic frequency.³⁰ Using a high-temperature value of 1860 K for the Debye temperature of diamond⁸ gives a Debye frequency of 1290 cm^{-1} . The highest observed acoustic frequency for diamond ranges from 1185 to 1191 cm^{-1} (longitudinal acoustic frequency at the X critical point = LA[X]), consistent with the value that best fits the data.

CONCLUSION

We measured the room temperature ultraviolet transmission of diamond and derived the absorption coefficient. Ultraviolet absorption at the band gap was characterized as an Urbach absorption edge model. We have also measured and characterized the weak absorption tail for this particular sample. Additionally, the room- and elevated-temperature transmission of diamond in the infrared has been measured. For the first time, four-phonon absorption was observed, and the temperature dependence of the two-, three-, and four-phonon absorption was determined. We have demonstrated that the general infrared absorption features of diamond can be duplicated by our multiphonon model, which was originally developed for highly ionic materials. Acoustic contributions to multiphonon absorption, which are important in the 10- μm spectral region, can also be modeled.

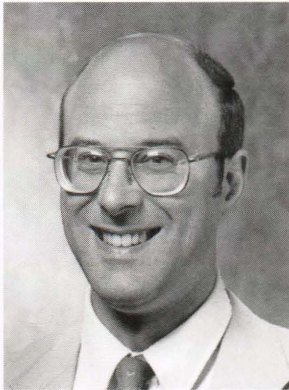
REFERENCES

- Strong, H. M., and Wentorf, R. H., "Growth of Large, High-Quality Diamond Crystals at General Electric," *Am. J. Phys.* **59**, 1005-1008 (1991).
- Yarbrough, W. A., and Messier, R., "Current Issues and Problems in the Chemical Vapor Deposition of Diamond," *Science* **247**, 688-696 (1990).
- Geis, M. W., and Angus, J. C., "Diamond Film Semiconductors," *Scientific American*, 84-89 (Oct 1992).
- Jiang, X., Harzer, J. V., Hillebrands, B., Wild, Ch., and Koidl, P., "Brillouin Light Scattering on Chemical-Vapor-Deposited Polycrystalline Diamond: Evaluation of the Elastic Moduli," *Appl. Phys. Lett.* **59**, 1055-1057 (1991).
- Morelli, D. T., Hartnett, T. M., and Robinson, C. J., "Phonon-Defect Scattering in High Thermal Conductivity Diamond Films," *Appl. Phys. Lett.* **59**, 2112-2114 (1991).
- Lu, G., and Swann, W. T., "Measurement of Thermal Diffusivity of Polycrystalline Diamond Film by the Converging Thermal Wave Technique," *Appl. Phys. Lett.* **59**, 1556-1558 (1991).
- Graeber, J. E., Jin, S., Kammlott, G. W., Herb, J. A., and Gardner, C. F., "Unusually High Thermal Conductivity in Diamond Films," *Appl. Phys. Lett.* **60**, 1576-1578 (1992).
- Field, J. E., *The Properties of Diamond*, Academic Press, San Diego (1979).
- Anthony, T. R., Banholzer, W. F., Fleischer, J. F., Wei, L., Kuo, P. K., et al., "Thermal Diffusivity of Isotopically Enriched ¹²C Diamond," *Phys. Rev. B* **42**, 1104-1111 (1990).
- Berman, R., Foster, E. L., and Ziman, J. M., "The Thermal Conductivity of Dielectric Crystals: The Effect of Isotopes," *Proc. Royal Soc. (London)* **A237**, 344-354 (1956).
- Berman, R., and Martinez, M., "The Thermal Conductivity of Diamonds," *Diamond Research 1976* (Suppl. to Ind. Diamond Rev.), 7-13 (1976).

- ¹²Johnson, C. E., Weimer, W. A., and Harris, D. C., "Characterization of Diamond Films by Thermogravimetric Analysis and Infrared Spectroscopy," *Mat. Res. Bull.* **24**, 1127-1134 (1989).
- ¹³Kaiser, W., and Bond, W. L., "Nitrogen, a Major Impurity in Common Type I Diamond," *Phys. Rev.* **115**, 857-863 (1959).
- ¹⁴Mykolajewycz, R., Kalnajs, J., and Smakula, A., "High-Precision Density Determination of Natural Diamonds," *J. Appl. Phys.* **35**, 1773-1778 (1964).
- ¹⁵Grimsditch, M. H., and Ramdas, A. K., "Brillouin Scattering in Diamond," *Phys. Rev. B* **11**, 3139-3148 (1975).
- ¹⁶Bundy, F. P., "Melting Point of Graphite at High Pressure: Heat of Fusion," *Science* **137**, 1055-1057 (1963).
- ¹⁷Victor, A. C., "Heat Capacity of Diamond at High Temperature," *J. Chem. Phys.* **36**, 1903-1911 (1962).
- ¹⁸Slack, G. A., and Bartram, S. F., "Thermal Expansion of Some Diamondlike Crystals," *J. Appl. Phys.* **46**, 89-98 (1975).
- ¹⁹Himpfel, F. J., Knapp, J. A., van Vechten, J. A., and Eastman, D. E., "Quantum Photoyield of Diamond(111)—A Stable Negative-Affinity Emitter," *Phys. Rev.* **B20**, 624-627 (1979).
- ²⁰Fontanella, J., Johnston, R. L., Colwell, J. H., and Andeen, C., "Temperature and Pressure Variation of the Refractive Index of Diamond," *Appl. Opt.* **16**, 2949-2951 (1977).
- ²¹Madelung, O. (ed.), *Semiconductors: Group IV Elements and III-V Compounds*, pp. 5-11, Berlin (1991).
- ²²Solin, S. A., and Ramdas, A. K., "Raman Spectrum of Diamond," *Phys. Rev. B* **1**, 1687-1698 (1970).
- ²³Namba, Y., Heidarpour, E., and Nakayama, M., "Size Effects Appearing in the Raman Spectra of Polycrystalline Diamonds," *J. Appl. Phys.* **72**, 1748-1751 (1992).
- ²⁴Peter, F., "Über Brechungsindizes und Absorptionkonstanten des Diamanten zwischen 644 und 226 μ ," *Z. Phys.* **15**, 358-368 (1923).
- ²⁵Edwards, D. F., and Ochoa, E., "Infrared Refractive Index of Diamond," *J. Opt. Soc. Am.* **71**, 607-608 (1981).
- ²⁶Rösch, S., "Die Optik des Fabulit, die Farbe des Brewsterwinkels und das Farbspielmoment," *Optica Acta* **12**, 253-260 (1965).
- ²⁷Ramachandran, G. N., "Thermo-optic Behavior of Solids: I. Diamond," *Proc. Ind. Acad. Sci.* **A25**, 266-279 (1947).
- ²⁸McNeely, J. R., Akerman, M. A., Clausing, R. E., McIntosh, M. B., Snyder, W. B., Thomas, M. E., and Linevsky, M. J., "High Temperature Optical Characterization of CVD Diamond," in *1992 Technical Digest from the OSA Annual Meeting*, Optical Society of America, Washington, D.C. Sep 1992.
- ²⁹Harris, K., Herrit, G. L., Johnson, C. J., Rummel, S. P., and Scarena, D. J., "Infrared Optical Characteristics of Type 2A Diamonds," *Appl. Opt.* **30**, 5015-5017 (1991), Erratum: *Appl. Opt.* **31**, 4342 (1992).
- ³⁰Klein, C. A., Hartnett, T. M., and Robinson, C. J., "Critical-Point Phonon Frequencies of Diamond," *Phys. Rev. B* **45**, 12,854-12,863 (1992).
- ³¹Thomas, M. E., Joseph, R. I., and Tropf, W. J., "Infrared Transmission Properties of Sapphire, Spinel, Ytria, and ALON as a Function of Frequency and Temperature," *Appl. Opt.* **27**, 239-245 (1988).
- ³²Sova, R. M., Linevsky, M. J., Thomas, M. E., and Mark, F. F., "High-Temperature Infrared Properties of Oxides," *Johns Hopkins APL Tech. Dig.* **13**, 368-378 (1992).
- ³³Thomas, M. E., and Joseph, R. I., "Optical Phonon Characterization of Diamond, Beryllia, and Cubic Zirconia," *Proc. SPIE* **1326**, 120-126 (1990).

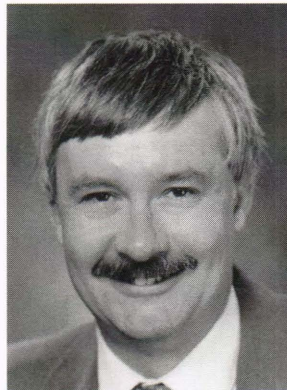
ACKNOWLEDGMENT: We wish to thank the U.S. Army Strategic Defense Command and Gail H. Lowe for supporting this work.

THE AUTHORS



MICHAEL E. THOMAS received a B.E.E. from the University of Dayton and an M.S. and Ph.D. from Ohio State University. He joined APL in 1979 and has been working on electromagnetic propagation and optical properties of materials. In 1982, he was a postdoctoral fellow in the Department of Physics, Naval Postgraduate School. In 1988, Dr. Thomas became a part-time G.W.C. Whiting School of Engineering faculty member, teaching courses on optical propagation and lasers. Current research interests include experimental and theoretical modeling of atmospheric propagation in

IR, DIAL, lidar, optical and IR window materials, and the IR properties of high-pressure gases. He has published over fifty book and journal articles in these fields. Dr. Thomas is a senior member of IEEE and holds membership in the Optical Society of America, SPIE, and Tau Beta Pi.



WILLIAM J. TROPF received a B.S. from The College of William and Mary (1968) and a Ph.D. from the University of Virginia (1973), both in physics. Dr. Tropf joined APL in 1977 and became a member of the Principal Professional Staff in 1981. Currently, he is supervisor of the Electro-Optical Systems Group in APL's Fleet Systems Department. His research interests are measuring and modeling the optical properties of materials, including developing a computer code recently licensed to Applied Research Corporation to predict optical properties as a function of wavelength and temperature. Dr. Tropf believes that understanding material properties is a key factor in developing high-performance systems. He has contributed to chapters on optical materials in the *Handbook of Optical Constants of Solids II*, *Electro-optics Handbook*, and the soon-to-be-published Optical Society of America *Handbook of Optics*, 2nd edition.